J Physiol 588.3 (2010) pp 465–478

Sodium accumulation promotes diastolic dysfunction in end-stage heart failure following *Serca2* knockout

William E. Louch[1,2], Karina Hougen[1,2], Halvor K. Mørk[1,2], Fredrik Swift[1,2], Jan M. Aronsen[1,2], Ivar Sjaastad[1,2,3], Henrik M. Reims[4], Borghild Roald[4], Kristin B. Andersson[1,2], Geir Christensen[1,2] and Ole M. Sejersted[1,2]

[1]*Institute for Experimental Medical Research,* [3]*Department of Cardiology and* [4]*Department of Pathology, Oslo University Hospital Ullevaal, Oslo, Norway*

[2]*Centre for Heart Failure Research, Faculty of Medicine, University of Oslo, Oslo, Norway*

Alterations in trans-sarcolemmal and sarcoplasmic reticulum (SR) Ca^{2+} fluxes may contribute to impaired cardiomyocyte contraction and relaxation in heart failure. We investigated the mechanisms underlying heart failure progression in mice with conditional, cardiomyocyte-specific excision of the SR Ca^{2+}-ATPase (SERCA) gene. At 4 weeks following gene deletion (4-week KO) cardiac function remained near normal values. However, end-stage heart failure developed by 7 weeks (7-week KO) as systolic and diastolic performance declined. Contractions in isolated myocytes were reduced between 4- and 7-week KO, and relaxation was slowed. Ca^{2+} transients were similarly altered. Reduction in Ca^{2+} transient magnitude resulted from complete loss of SR Ca^{2+} release between 4- and 7-week KO, due to loss of a small remaining pool of SERCA2. Declining SR Ca^{2+} release was partly offset by increased L-type Ca^{2+} current, which was facilitated by AP prolongation in 7-week KO. Ca^{2+} entry via reverse-mode Na^+–Ca^{2+} exchange (NCX) was also enhanced. Up-regulation of NCX and plasma membrane Ca^{2+}-ATPase increased Ca^{2+} extrusion rates in 4-week KO. Diastolic dysfunction in 7-week KO resulted from further SERCA2 loss, but also impaired NCX-mediated Ca^{2+} extrusion following Na^+ accumulation. Reduced Na^+-K^+-ATPase activity contributed to the Na^+ gain. Normalizing $[Na^+]$ by dialysis increased the Ca^{2+} decline rate in 7-week KO beyond 4-week values. Thus, while SERCA2 loss promotes both systolic and diastolic dysfunction, Na^+ accumulation additionally impairs relaxation in this model. Our observations indicate that if cytosolic Na^+ gain is prevented, up-regulated Ca^{2+} extrusion mechanisms can maintain near-normal diastolic function in the absence of SERCA2.

(Received 20 October 2009; accepted after revision 5 December 2009; first published online 14 December 2009)

Corresponding author W. E. Louch: Institute for Experimental Medical Research, 4.etg. Kirurgisk Bygning, Oslo University Hospital Ullevaal, 0407 Oslo, Norway. Email: w.e.louch@medisin.uio.no

Abbreviations AP, action potential; $[Ca^{2+}]_i$, intracellular $[Ca^{2+}]$; FF, *Serca2*$^{flox/flox}$ mice; HF, heart failure; KO, *Serca2*$^{flox/flox}$ Tg(αMHC-MerCreMer) mouse; LAD, left atrial diameter; LV, left ventricular; $[Na^+]_i$, intracellular $[Na^+]$; NCX, Na^+–Ca^{2+} exchanger; NKA, Na^+-K^+-ATPase; PMCA, plasmalemmal Ca^{2+}-ATPase; SERCA, SR Ca^{2+}-ATPase; SR, sarcoplasmic reticulum.

Introduction

Contraction in adult ventricular myocytes is triggered by a transient increase in intracellular $[Ca^{2+}]$ ($[Ca^{2+}]_i$) during the action potential (AP). This rise in $[Ca^{2+}]_i$ results from Ca^{2+} influx through L-type Ca^{2+} channels, which in turn triggers release of a much larger amount of Ca^{2+} from the sarcoplasmic reticulum (SR) (Bers, 2001). Relaxation occurs as Ca^{2+} is recycled into the SR by the SR Ca^{2+}-ATPase (SERCA) and as Ca^{2+} is extruded from the cell, primarily by the Na^+–Ca^{2+} exchanger (NCX).

Altered cardiomyocyte Ca^{2+} homeostasis is believed to be an important mechanism underlying heart failure (HF), and may contribute to both systolic and diastolic dysfunction in this condition. Systolic dysfunction results, at least in part, from reduced magnitude of Ca^{2+} transients due to lower Ca^{2+} content of the SR (Bers, 2006). Reduced SR content is believed to be caused by depressed SERCA function and greater diastolic SR Ca^{2+} leak. Increased expression and function of the NCX may also impair SR Ca^{2+} reuptake since NCX competes with SERCA for extrusion of Ca^{2+} from the cytosol (Pogwizd *et al.*

DOI: 10.1113/jphysiol.2009.183517

2001). Less is known about the cellular mechanisms that underlie diastolic HF. However, Hasenfuss *et al.* (1999) observed that hearts from human HF patients with diastolic dysfunction had decreased SERCA expression but unchanged NCX. In contrast, patients with preserved diastolic function exhibited increased NCX levels. Thus, alterations in the relationship between trans-SR and trans-sarcolemmal Ca^{2+} fluxes may be critical in determining diastolic function in the failing heart, and progression to end-stage failure. The ability to increase transport of Ca^{2+} and Na^{+} across the sarcolemma may be an important compensatory mechanism for reduction in SR function, and a progressive decline in this ability may cause deterioration of diastolic function in HF patients.

We recently investigated the consequences of SERCA down-regulation in adult mice with cardiomyocyte-specific, conditional excision of the *Serca2* gene (Andersson *et al.* 2009*a*). SERCA protein expression declined rapidly following gene deletion, and was below 5% of control values after 4 weeks. Surprisingly, we observed only moderately impaired cardiac performance with a relatively minor reduction in both systolic and diastolic function (Andersson *et al.* 2009*a*). Cardiomyocytes were observed to compensate for loss of SR function by increasing Ca^{2+} cycling across the sarcolemma. In the present study, we examine the cellular mechanisms underlying the eventual progression to end-stage HF in these mice. Our results indicate that while reduction of SR function following SERCA loss contributes to both systolic and diastolic dysfunction, impaired relaxation also results from slowing of NCX-mediated Ca^{2+} extrusion due to cytosolic Na^{+} accumulation. Importantly, we show that when such Na^{+} increases are prevented, up-regulated Ca^{2+} extrusion mechanisms can maintain near-normal diastolic function in the complete absence of a functional SR.

Methods

Ethical approval

The investigation was approved by the Norwegian National Committee for Animal Welfare under the Norwegian Animal Welfare Act, which conforms to the *Guide for the Care and Use of Laboratory Animals* published by the US National Institutes of Health (NIH publication No. 85-23, revised 1996), and ethical guidelines from *The Journal of Physiology* (Drummond, 2009).

Animal care

The *Serca2*$^{flox/flox}$ Tg(αMHC-MerCreMer) mouse (KO) employed in our experiments allows for inducible, cardiomyocyte-specific disruption of the *Serca2* gene in adult mice (Andersson *et al.* 2009*a*). *Serca2* gene excision in 8- to 10-week-old mice was accomplished by inclusion of tamoxifen base powder (RM1 FG SQC, 811004, Scanbur BK) in the feed ($100\,mg\,(200\,g)^{-1}$) for 7 days (Andersson *et al.* 2009*c*). *Serca2*$^{flox/flox}$ mice (FF) served as controls (Andersson *et al.* 2009*a*,*b*) and were subjected to the same feeding regime. Tamoxifen administration results in *Serca2* gene excision exclusively in the cardiomyocytes of KO animals (Andersson *et al.* 2009*a*). A total of 171 anaesthetized (~2% isoflurane) mice were killed by cervical dislocation, and hearts were harvested at 4 and 7 weeks following tamoxifen administration. Echocardiographic characterization of heart function was performed on anaesthetised (~2% isoflurane), self-breathing mice (Andersson *et al.* 2009*a*).

Histology

Following fixation in 4% formaldehyde, hearts were transected at the midventricular level, routinely processed and embedded in paraffin. Serial 3.5 μm sections were stained with haematoxylin and eosin, acid fuchsin orange G (AFOG) and van Gieson stains, and were assessed blindly by two investigators. The degree of fibrosis in each heart was given a score on a scale of 0–3.

Western blotting

Protein levels were determined by Western blot as described in Andersson *et al.* (2009*a*) but with images detected by a LAS-4000 Mini CCD detection system (Fujifilm, Tokyo, Japan). Antibodies used for protein detection were: SERCA2a (MA3-919), L-type Ca^{2+} channel $\alpha_2\delta_1$ subunit (MA3-921), pan-plasmalemmal Ca^{2+}-ATPase (PMCA, MA3-914) (all Affinity BioReagents, Golden, CO, USA), NCX1 (Thomas *et al.* 2003), Na^{+}–K^{+}-ATPase (NKA) α_2 isoforms (Millipore, Billerica, MA, USA), and L-type Ca^{2+} channel α_{1C} subunit (AAC-003, Alomone Laboratories, Jerusalem, Israel). SERCA2b antiserum (Campbell *et al.* 1993) was the kind gift of Frank Wuytack, Katholieke Universiteit Leuven, Leuven, Belgium. Calsequestrin was used as loading control.

Ca^{2+}-ATPase content

Total left ventricular (LV) Ca^{2+}-ATPase was quantified as thapsigargin-sensitive calcium-dependent incorporation of [^{32}P] using whole-tissue homogenates and [γ^{32}P]ATP (Everts *et al.* 1989; Andersson *et al.* 2009*a*).

Cardiomyocyte experiments

Cardiomyocytes were enzymatically isolated (Andersson *et al.* 2009*a*) and placed in a perfusion chamber on the stage of an inverted microscope. Experiments were performed at 37°C. Basic cell shortening and Ca^{2+} transient measurements were recorded during field stimulation (3 ms biphasic pulse, 25% above threshold) during superfusion with Hepes Tyrode solution containing (in mM): 140 NaCl, 1 $CaCl_2$, 0.5 $MgCl_2$, 5.0 Hepes, 5.5 glucose, 0.4 NaH_2PO_4 and 5.4 KCl (pH 7.4). Contractions were measured using a video edge detector (Crescent Electronics, Sandy, UT, USA) coupled to a television monitor. Ca^{2+} transients were recorded in fluo-4 AM (Invitrogen Molecular Probes, Eugene, OR, USA) loaded myocytes using an LSM 510 confocal microscope (Zeiss GmbH, Jena, Germany) in line-scan mode (Louch *et al.* 2006). Time constants (τ) and rate constants (defined as $1/\tau$) were calculated from single exponential fits of Ca^{2+} transient decays (Mork *et al.* 2009). Time to 50% decline was measured in experiments with very slow changes in $[Ca^{2+}]_i$ which were difficult to fit exponentially.

Diastolic $[Ca^{2+}]_i$ was determined by whole-cell photometry (Photon Technology International, Monmouth Junction, NJ, USA) in cells pipette-loaded with a solution containing (in mM): 0.1 fura-2 salt (Invitrogen Molecular Probes), 120 potassium aspartate, 0.5 $MgCl_2$, 10 NaCl, 0.06 EGTA, 10 Hepes, 10 glucose, 25 KCl and 4 K_2-ATP (pH 7.2). Fura-2 fluorescence ratios (F_{340}/F_{380}) were calibrated to $[Ca^{2+}]_i$, and calculated diastolic values were then used to calibrate Ca^{2+} transients recorded in fluo-4-loaded cells (Cheng *et al.* 1993; Andersson *et al.* 2009*a*).

Patch-clamp experiments were conducted with an Axoclamp 2B amplifier (Axon Instruments, Foster City, CA, USA), pCLAMP software (Axon Instruments) and low resistance pipettes (1–2 MΩ). AP recordings were made in bridge-mode, and representative tracings employed as voltage-clamp waveforms as described (Mork *et al.* 2009). L-type Ca^{2+} current was recorded during APs in Na^+- and K^+-free internal (in mM: 135 $CsCl_2$, 3 Mg-ATP, 5 EGTA and 10 Hepes) and external (in mM: 136 TEA-Cl, 1.1 $MgCl_2$, 10 glucose, 10 Hepes, 4 KCl and 1 $CaCl_2$) solutions, and calculated as the current sensitive to 20 μM nifedipine (Mork *et al.* 2009). L-type Ca^{2+} current was also recorded during depolarizing 200 ms voltage steps from −50 mV, with an internal solution containing (in mM) 130 CsCl, 0.33 $MgCl_2$, 4 Mg-ATP, 0.06 EGTA, 10 Hepes and 20 TEA, and an extracellular solution containing (in mM) 20 CsCl, 1 $MgCl_2$, 135 NaCl, 10 Hepes, 10 D-glucose, 4 4-aminopyridine and 1 $CaCl_2$ (Andersson *et al.* 2009*a*).

Intracellular Na^+ concentration ($[Na^+]_i$) was assessed in myocytes loaded with SBFI AM as described previously (Swift *et al.* 2007 & Baartscheer *et al.* 1997). Total NKA current was obtained by rapidly elevating extracellular $[K^+]$ from 0 mM to 5.4 mM (Baartscheer *et al.* 1997; Swift *et al.* 2007). The α_2 NKA isoform component of the total current was calculated as the difference current following treatment with 5 μM ouabain, which selectively blocks the α_2 isoform (Berry *et al.* 2007). Remaining current was attributed to the α_1 isoform.

Statistics

Data are expressed as mean values ± S.E.M. Statistical significance was calculated using paired or unpaired *t* tests. *P* values < 0.05 were considered significant.

Results

Development of end-stage HF

Kaplan Meyer survival curves (Fig. 1*A*) indicated that KO mice died over a period of 3.4 weeks, starting at 6.9 weeks following induction of *Serca2* gene deletion by tamoxifen. KO mice were killed at 7 weeks (7-week KO) in further experiments due to ethical considerations. To examine the phenotype and mechanisms of HF development, data from 7-week KO were compared with the 4 week time point (4-week KO). Cardiac output was reduced in 7-week, but not 4-week KO (Fig. 1*B*), as we have observed previously (Andersson *et al.* 2009*a*). Similarly, left atrial diameter (LAD), a sensitive parameter for congestive HF in mice (Finsen *et al.* 2005), was increased between 4-week and 7-week KO (Fig. 1*C*, $P < 0.05$ within KO). Lung weight/body weight ratios also indicated greater pulmonary congestion in 7-week KO than 4-week KO (167% *vs.* 130% of FF values, $P < 0.05$, Table 1). Tissue Doppler measurements showed that HF development involved impairment of both systolic and diastolic function (Fig. 1*D* and *E*, respectively). We also observed depressed heart rate in KO mice (Table 1), which we believe resulted from *Serca2* ablation in the sinoatrial node (Andersson *et al.* 2009*a*).

LV weight/body weight ratios and LV myocyte dimensions were similar in FF and KO at both time points (Table 1), indicating that LV hypertrophy was not present in KO. Histological examination of heart sections showed no evidence of inflammatory cell infiltration, generalized myocyte degeneration or disarray in KO hearts (Fig. 1*F*). However, a modest degree of fibrosis was observed with no apparent progression between the two time points (mean score = 1.3 ± 0.5 in 4-week KO *vs.* 1.3 ± 0.8 in 7-week KO, P = NS). Since we could not detect time-dependent alterations in LV geometry or histology, we hypothesized that HF progression in KO resulted from declining systolic and diastolic cardiomyocyte function.

Isolated myocyte contractions and Ca^{2+} transients

Representative myocyte contraction recordings during 1 Hz stimulation are shown in Fig. 2*A*. Contraction

magnitude was reduced in 4-week KO from 4-week FF values, and further decreased in 7-week KO (Fig. 2*B*). Cardiomyocyte relaxation was also progressively slowed between 4-week and 7-week KO cells (Fig. 2*C*). Similar changes were observed in Ca^{2+} transients (Fig. 2*D*). Mean transient magnitude was markedly decreased in 4-week KO myocytes, and further decreased in 7-week KO (Fig. 2*E*). The declining phase of the Ca^{2+} transient was progressively slowed in KO cells (Fig. 2*F*).

Increasing stimulation frequency to 6 Hz increased contraction magnitude to near-normal values in 4-week KO (Table 1). In 7-week KO, cell shortening was also improved by increasing the stimulation rate (1 Hz, 14% FF; 6 Hz, 48% FF, $P < 0.05$), but mean measurements remained significantly below control values. Similarly, relaxation kinetics were improved in both KO groups at higher stimulation frequency, but remained more markedly below FF values in 7-week KO (25% FF *vs.* 47% FF in 4-week KO, $P < 0.05$, Table 1). Thus, during stimulation in the physiological frequency range, myocyte contraction magnitude and relaxation kinetics roughly paralleled *in vivo* measurements of systolic and diastolic function. While we observed important differences in contraction amplitudes with frequency, Ca^{2+} transient amplitudes were similarly depressed in KO myocytes at 1 and 6 Hz (4-week KO: 25 ± 4%, 27 ± 4% FF, respectively; 7-week KO: 15 ± 2%, 16 ± 3% FF, P = NS for 1 Hz *vs.* 6 Hz, $P < 0.05$ for 4-week *vs.* 7-week KO). Diastolic $[Ca^{2+}]_i$ in KO was not altered from FF values at either time point or frequency (data not shown).

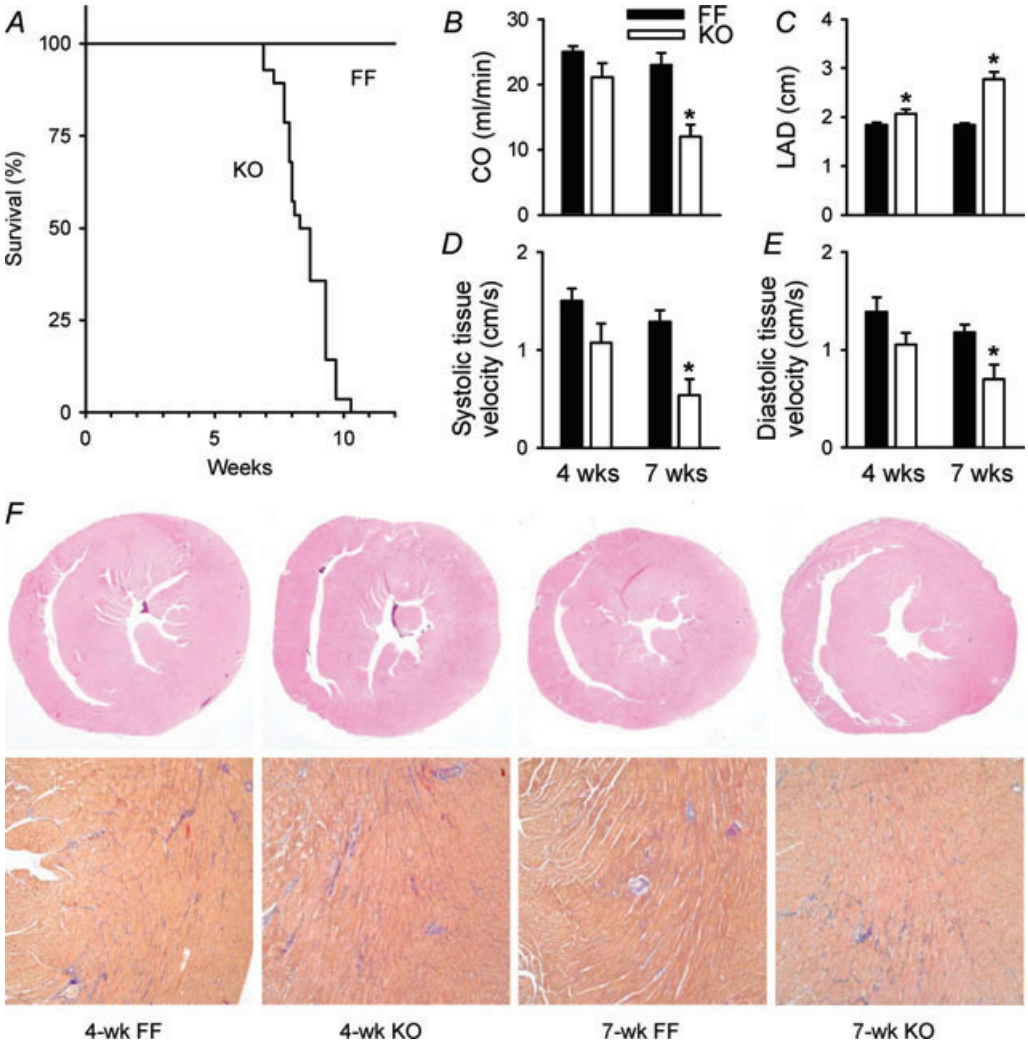

Figure 1. Progression to end-stage HF in KO mice involved impairment of systolic and diastolic function
A, survival curves (FF, $n = 26$; KO, $n = 27$). Echocardiographic measurements of cardiac output (*B*), left atrial diameter (*C*), systolic tissue velocity (*D*), and diastolic tissue velocity (*E*) (FF, $n = 6$; KO, $n = 5$). *F*, whole heart histological sections at 20× (top panels, hematoxylin/eosin) and 100× magnification (bottom panels, AFOG, with blue staining indicating fibrosis). *$P < 0.05$ *vs.* equivalent FF.

Table 1. Animal and cell characteristics

	4-week FF	4-week KO	7-week FF	7-week KO
Age (weeks)	14.0 ± 0.1	13.9 ± 0.2	17.1 ± 0.1	16.8 ± 0.2
Heart rate (min^{-1})	487 ± 18	433 ± 24*	498 ± 19	395 ± 11*
BW (g)	23.7 ± 0.6	26.4 ± 0.7*	27.0 ± 0.7	24.6 ± 0.7*
LVW (mg)	75.7 ± 2.4	87.5 ± 2.7*	89.0 ± 3.0	83.5 ± 3.0
LW (mg)	134 ± 2	182 ± 6*	153 ± 5	232 ± 9*
LVW/BW	3.2 ± 0.1	3.3 ± 0.0	3.3 ± 0.0	3.4 ± 0.1
LW/BW	5.4 ± 0.3	7.0 ± 0.2*	5.7 ± 0.2	9.5 ± 0.4*
Cell length (μm)	129.6 ± 1.8	127.6 ± 1.8	127.6 ± 1.7	131.9 ± 1.9
Cell width (μm)	22.0 ± 0.4	21.8 ± 0.4	22.2 ± 0.4	21.5 ± 0.3
Fract. short. at 6 Hz (%)	3.76 ± 0.54	2.92 ± 0.43	2.98 ± 0.32	1.43 ± 0.11*
dl/dt_{min} at 6 Hz ($\mu m\ ms^{-1}$)	0.101 ± 0.020	0.048 ± 0.007*	0.075 ± 0.010	0.019 ± 0.004*

BW, body weight; LVW, left ventricular weight; LW, lung weight; Fract. short. , fractional shortening, $^*P < 0.05$ *vs.* FF; $n_{animals}$: 4-week FF = 29, 4-week KO = 32; 7-week FF = 35; 7-week KO = 25; n_{cells} (length/width): 4-week FF = 115, 4-week KO = 121; 7-week FF = 139; 7-week KO = 143; n_{cells} (6 Hz function): 4-week FF = 13, 4-week KO = 13, 7-week FF = 15, 7-week KO = 11.

Declining SR function

We examined changes in cellular Ca^{2+} fluxes underlying alterations in Ca^{2+} transients and contraction/relaxation in KO myocytes. Ca^{2+} release elicited by rapid application of 10 mM caffeine was reduced to 27% of FF values in 4-week KO and 4% in 7-week KO, indicating declining SR Ca^{2+} content (Fig. 3*A* and *B*). To estimate SR Ca^{2+} release during each beat, we compared steady-state Ca^{2+} transients in the presence and absence of caffeine (Andersson *et al.* 2009*a*) (Fig. 3*D*). In FF cells, Ca^{2+} transient amplitudes were markedly reduced during

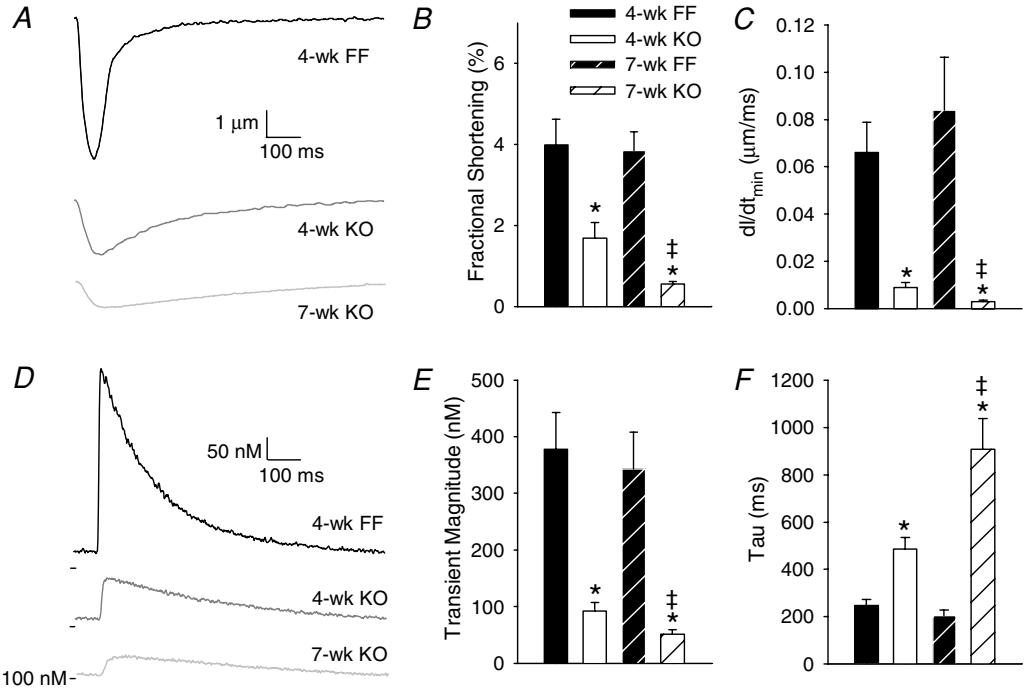

Figure 2. Contractions and Ca^{2+} transients became progressively smaller and slower to decline in KO cardiomyocytes

A, representative contraction traces, from isolated myocytes during 1 Hz field stimulation. Mean fractional shortening (*B*) and maximum relaxation velocity measurements (*C*). Representative Ca^{2+} transients recorded by fluo-4 fluorescence (*D*). Mean Ca^{2+} transient magnitudes (*E*) and decay kinetics (*F*). (*n* for panels *B* and *C*, *E* and *F*: 4-week FF = 13, 16; 4-week KO = 13, 20; 7-week FF = 15, 19; 7-week KO = 11, 19; $^*P < 0.05$ *vs.* equivalent FF, ‡$P < 0.05$ *vs.* equivalent 4-week).

caffeine, confirming that the Ca^{2+} transient was predominantly derived from SR (Fig. 3*E*). In contrast, SR Ca^{2+} release was minute in 4-week KO (11% FF values), and was not detectable in 7-week KO. Similarly, calculated rate constants for SR Ca^{2+} re-uptake were markedly reduced in 4-week KO, and were not significantly different from zero in 7-week KO (Fig. 3*F*). Using the measurements of SR-dependent and caffeine-elicited Ca^{2+} transients, we estimated that fractional release was reduced to $21 \pm 3\%$ in 4-week KO compared with $51 \pm 10\%$ in 4-week FF controls ($P < 0.05$). Very low SERCA2a expression levels were observed in 4-week KO; however, a small but significant further down-regulation was observed in 7-week KO (Fig. 3*C*). SERCA2b expression was also markedly reduced in KO, but similar in 4-week and 7-week cells ($10 \pm 1\%$ and $10 \pm 1\%$ FF values, respectively, $P =$ NS). Although Western blot sensitivity is below optimal at low protein expression levels, a reduction in SERCA2a levels between 4- and 7-week KO could account for declining SR function. Indeed, we observed that thapsigargin-sensitive Ca^{2+}-ATPase content in whole-heart homogenates was reduced from $15.8 \pm 3.0\%$ to $7.9 \pm 1.6\%$ of FF values between 4-week and 7-week KO ($P < 0.05$). Also, the small degree of SR function present in 4-week KO cells was blocked by 1 μM thapsigargin, as caffeine-elicited transients were reduced to 4 ± 4 nM (*vs.* 167 ± 42 nM in untreated, $P < 0.05$) and SR Ca^{2+} release did not occur (data not shown). Seven-week KO transient magnitudes were unaffected by thapsigargin application (23 ± 4 nM *vs.* 26 ± 4 nM in untreated, $P =$ NS). Thus, very low SERCA levels appear capable of partially refilling the SR in 4-week KO myocytes, and this residual SERCA activity is lost by the 7-week time point.

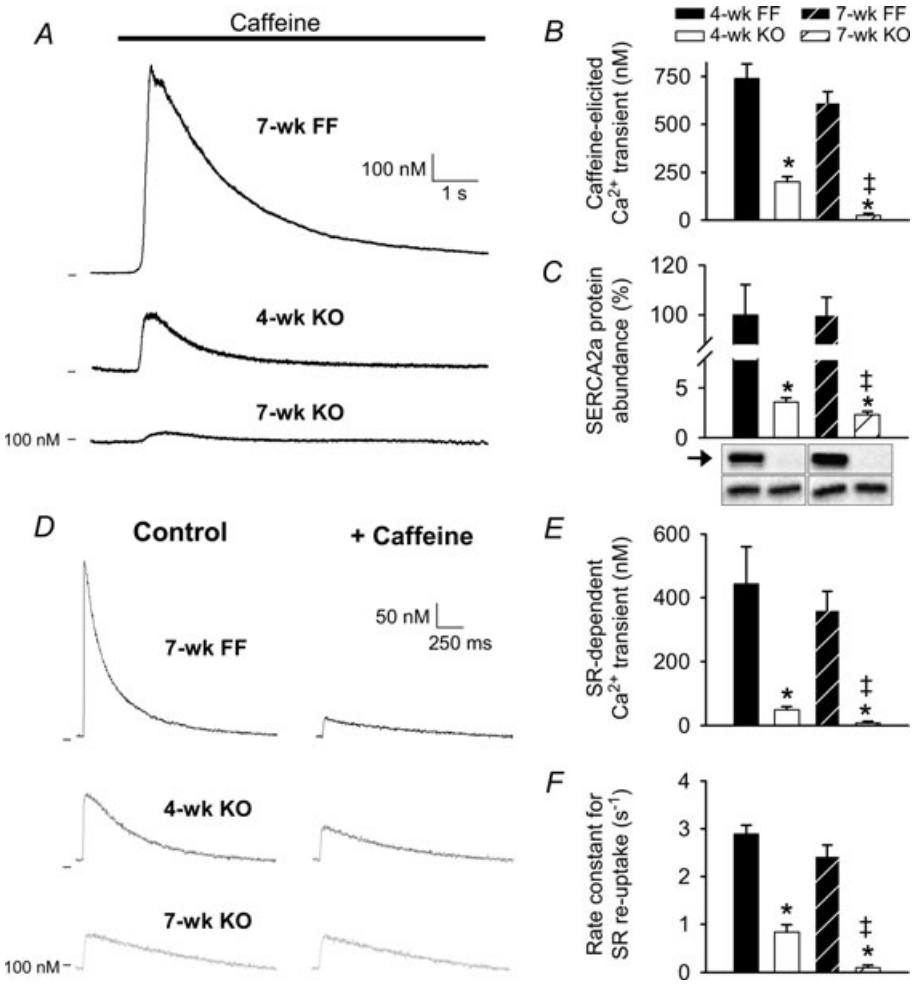

Figure 3. Minute SR function was present in 4-week, but not 7-week KO
Representative caffeine-elicited Ca^{2+} transients (*A*) and magnitude measurements (*B*). Expression levels of SERCA2a (arrow) *vs.* calsequestrin (lower bands) (*C*). SR Ca^{2+} release during each beat was assessed by comparing Ca^{2+} transients in the presence and absence of caffeine (*D*). SR Ca^{2+} release (*E*) and reuptake (*F*). (*n* for panels *B* and *C*, *E* and *F*: 4-week FF = 13, 5, 9; 4-week KO = 20, 6, 19; 7-week FF = 20, 6, 18; 7-week KO = 19, 7, 19; $^*P < 0.05$ *vs.* equivalent FF, ‡$P < 0.05$ *vs.* equivalent 4-week).

Enhanced Ca^{2+} influx

Representative recordings of L-type Ca^{2+} currents during voltage-clamp steps are shown in Fig. 4*A*. Mean measurements of peak current in 4-week and 7-week KO were 140% and 149% of FF values, respectively ($P < 0.05$ *vs.* FF, $P =$ NS within KO). No marked shift in the current–voltage relationship was observed. Slower Ca^{2+} current decay kinetics in KO (half-decay time: 4-week FF $= 4.7 \pm 0.2$ ms, 4-week KO $= 8.5 \pm 0.8$ ms $P < 0.05$, 7-week FF $= 5.6 \pm 0.5$ ms, 7-week KO $= 8.6 \pm 0.9$ ms $P < 0.05$) resulted in very large integrated Ca^{2+} currents, especially in 7-week KO (4-week KO = 188% FF, 7-week KO = 220% FF, $P =$ NS within KO, Fig. 4*B*). Parallel alterations were observed in L-type Ca^{2+} channel expression. Levels of the pore-forming subunit, α_{1C}, were 146% of FF values in 4-week KO (Fig. 4*C*), and there was a strong tendency for further up-regulation in 7-week KO (178% FF). Levels of the α_2/δ_1 regulatory subunit were also increased to $133 \pm 10\%$ and $147 \pm 10\%$ of FF levels in 4-week and 7-week KO, respectively (data not shown; $P =$ NS within KO).

We examined whether alterations in AP configuration might additionally modify L-type Ca^{2+} influx and the Ca^{2+} transient. Representative recordings (Fig. 5*A*) and mean data (Fig. 5*B*) show that APs were prolonged at 50% and 70% repolarization in 7-week KO. Resting membrane potential and transient outward K^+ current measurements were similar in all groups (data not shown), suggesting that AP prolongation in KO resulted primarily from augmented Ca^{2+} current. Also, AP prolongation was not observed in 7-week KO during treatment with 20 μM nifedipine (data not shown). The representative APs shown in Fig. 5*A* were employed as voltage-clamp waveforms in 7-week FF and 7-week KO cells. Figure 5*C* and *D* show that steady-state stimulation with the KO AP resulted in a larger Ca^{2+} transient than stimulation with the FF AP. This difference in amplitude was small in absolute terms (27 nM in 7-week FF cells, 14 nM in 7-week KO cells, $P =$ NS), but proportionally very large in KO

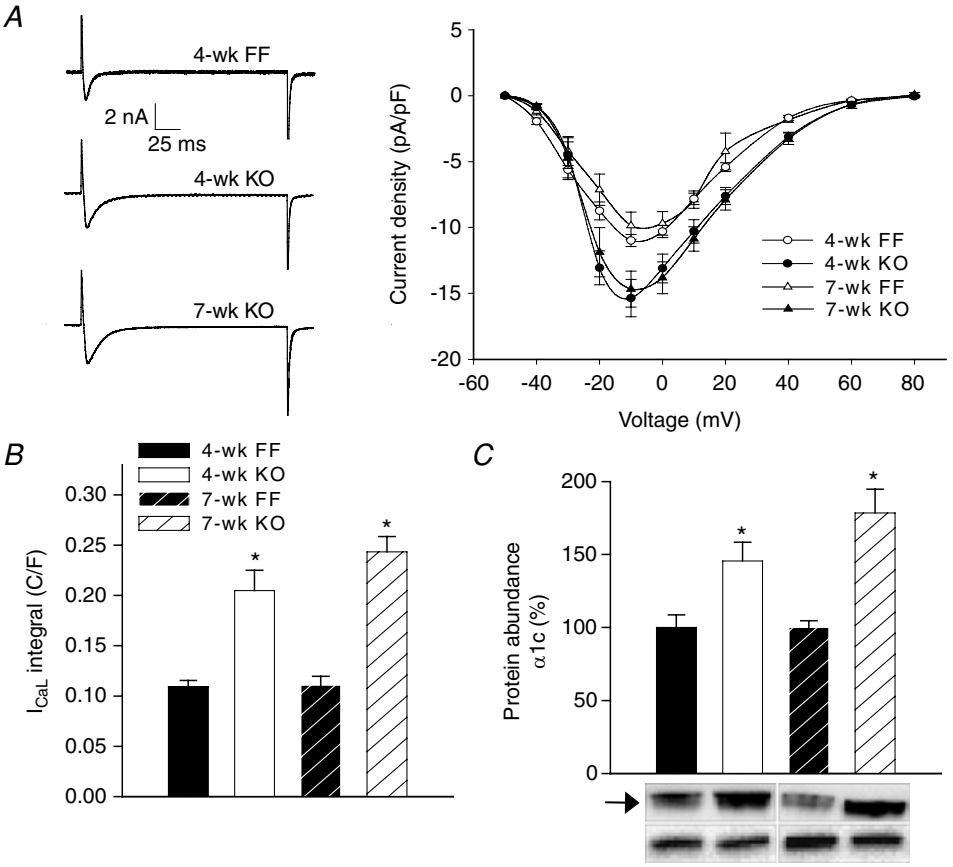

Figure 4. Increased L-type Ca^{2+} current in KO myocytes
A, representative L-type Ca^{2+} currents recorded during a voltage step from −50 mV to −10 mV (left panel). L-type current–voltage relationship (right panel). *B*, integrated current measurements during the step to –10 mV. *C*, protein levels of the Ca^{2+} channel α_{1C} subunit (arrow) *vs.* calsequestrin (lower bands). (*n* for panels *A* and *B*, and *C*: 4-week FF = 14, 5; 4-week KO = 12, 6; 7-week FF = 8, 6; 7-week KO = 13, 7; $^*P < 0.05$ *vs.* equivalent FF).

(% increase, 67% *vs.* 19% in FF, $P < 0.05$). In 7-week KO myocytes, where the entire transient results from Ca^{2+} influx, augmentation of transients during the KO AP predominantly resulted from a 43% increase in integrated L-type Ca^{2+} current (Fig. 5*E*). Thus, overall L-type Ca^{2+} entry in 7-week KO was dramatically increased from 7-week FF values by approximately 3- to 3.5-fold, when AP alterations were considered (Fig. 5*E*). This indicates that AP alterations can be an important compensatory mechanism for augmenting Ca^{2+} influx when SR function is inhibited.

NCX-mediated Ca^{2+} entry was also examined in 7-week FF and KO, by treating myocytes with 5 μM KB-R7943 (Tocris/Bio Nuclear AB, Bromma, Sweden) to preferentially block reverse-mode function (Iwamoto *et al.* 1996; Satoh *et al.* 2000). KB-R7943 treatment did not alter Ca^{2+} transient magnitude in 7-week FF cells (134 ± 23 nM *vs.* 140 ± 23 nM in untreated, $P =$ NS), but

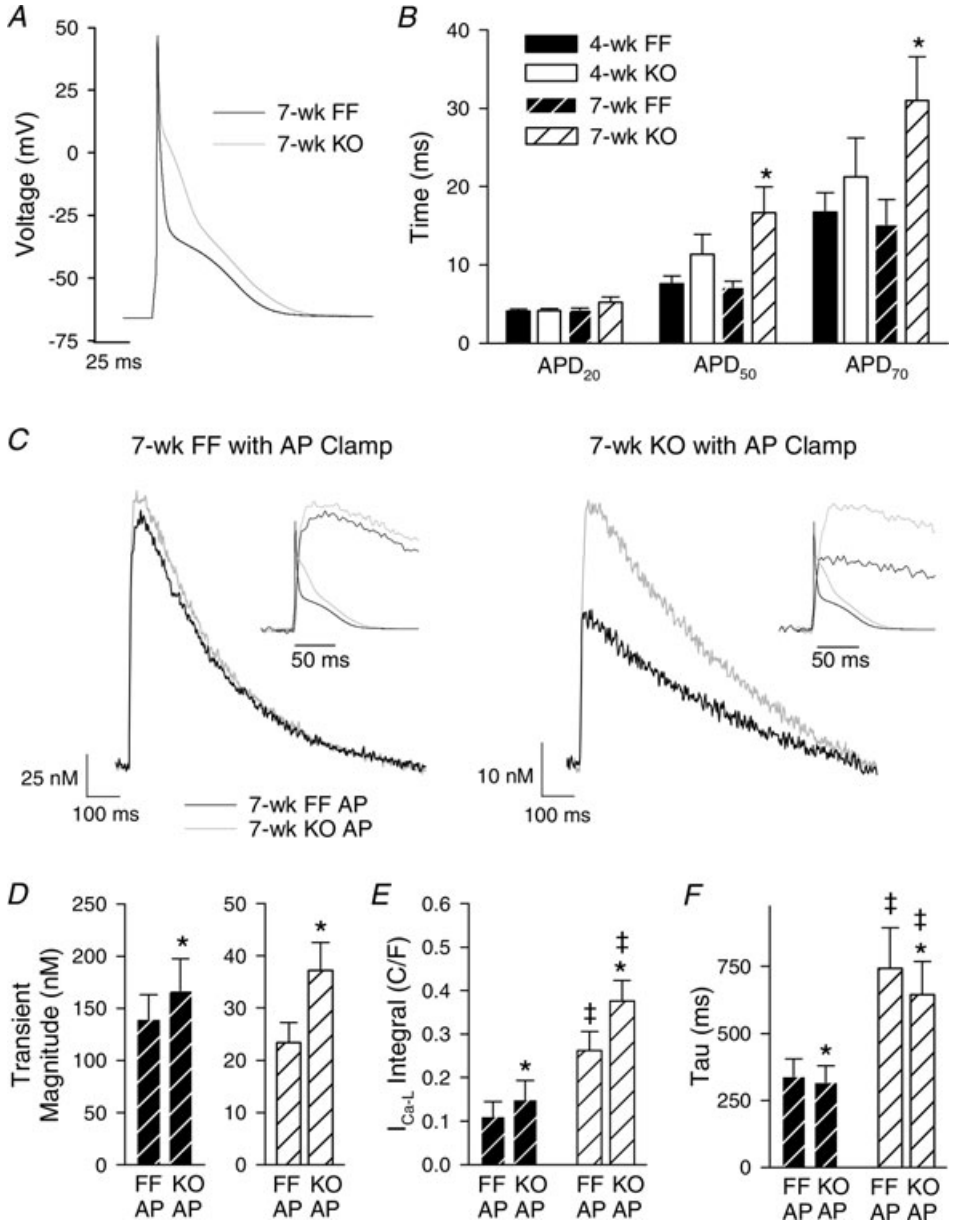

Figure 5. AP prolongation facilitated Ca^{2+} entry in 7-week KO
A, representative AP recordings at 1 Hz. *B*, times to 20%, 50% and 70% repolarization (APD_{20}, APD_{50} and APD_{70}) ($n = 16, 17, 11, 16$; $^*P < 0.05$ *vs.* corresponding FF). *C*, representative Ca^{2+} transients recorded during voltage-clamp stimulation with AP waveforms from *A*. Insets illustrate an expanded time scale with APs superimposed. Transient magnitude (*D*), integrated L-type Ca^{2+} current (*E*), and decay kinetics of the Ca^{2+} transient (*F*). (*n* for panels *D*, *E* and *F*: 7-week FF = 9, 8, 9; 7-week KO = 12, 4, 12; $^*P < 0.05$ *vs.* equivalent FF AP, ‡$P < 0.05$ *vs.* equivalent 7-week FF).

markedly reduced transient size in 7-week KO (14 ± 2 nM *vs.* 23 ± 4 nM in untreated, $P < 0.05$). This suggests that the Ca^{2+} transient in 7-week KO is supported by enhanced NCX-mediated Ca^{2+} entry, in addition to increased L-type Ca^{2+} current (described above). Reverse-mode NCX function might be expected to be further facilitated by AP prolongation. However, switching between the FF and KO AP stimulus during KB-R7943 treatment augmented Ca^{2+} transients (increase of 17 ± 8% in 7-week FF, 67 ± 10% in 7-week KO, $P < 0.05$) to a similar extent as was observed in untreated cells (Fig. 5*D*). Thus, the prolonged AP in 7-week KO predominantly amplifies Ca^{2+} transients by increasing L-type current.

Ca^{2+} extrusion: compensation and de-compensation

We investigated whether alterations in Ca^{2+} extrusion contributed to slowing of Ca^{2+} transient decline during development of diastolic dysfunction between 4- and 7-week KO. Decay kinetics were examined for transients recorded in the presence of caffeine (as in Fig. 3*D*), when Ca^{2+} removal is dependent solely on trans-sarcolemmal flux. Representative Ca^{2+} transients (Fig. 6*A*) and mean data (Fig. 6*B*) show that while Ca^{2+} extrusion was more rapid than FF in 4-week KO, extrusion was slowed to control values in 7-week KO. By comparing rate constants of Ca^{2+} reuptake and extrusion, we can calculate that 60% of the overall slowing of Ca^{2+} transient decline between 4-week and 7-week KO resulted from loss of SR re-uptake, while the remaining 40% resulted from slowing of Ca^{2+} extrusion. Importantly, slowing of extrusion in KO occurred despite a progressive up-regulation in NCX and PMCA protein levels between 4 and 7 weeks (Fig. 6*C*).

In AP clamp experiments, we observed that the 7-week KO AP did not alter Ca^{2+} transient decline (Fig. 5*F*), since even the prolonged AP was repolarized shortly after the transient peak (insets in Fig. 5*C*). We hypothesized that slowing of Ca^{2+} extrusion instead resulted from inhibition of forward-mode NCX function by elevation of $[Na^+]_i$. Indeed, SBFI ratios were increased in 7-week myocytes, indicating cytosolic Na^+ accumulation (Fig. 7*A*). Interestingly, this was associated with reduced expression levels of NKA α_1 and α_2 isoforms (Fig. 7*B*). Total NKA current was also reduced in 7-week KO, which included a 40% reduction in α_2 current and a tendency for decreased α_1 current (Fig. 7*C*). We have previously shown that reduced NKA activity increases $[Na^+]_i$ (Swift *et al.* 2007). As proof of principle that such changes can also impair Ca^{2+} extrusion, we examined Ca^{2+} removal during NKA blockade by ouabain. In 7-week FF cells, ouabain significantly slowed the half-decay time of Ca^{2+} transients recorded during caffeine (Fig. 7*D*). Ouabain treatment did not, however, slow Ca^{2+} extrusion in 7-week KO, suggesting that baseline elevations in $[Na^+]_i$ may have maximally inhibited NCX function. Interestingly, Ca^{2+} extrusion during ouabain was more rapid in 7-week KO than FF, which probably resulted from the marked up-regulation of PMCA protein expression in KO.

To further investigate the importance of elevated $[Na^+]_i$ for slowing of Ca^{2+} extrusion, we examined Ca^{2+} transients in cells dialysed with patch pipettes containing a low $[Na^+]$ (6 mM). Figure 7*E* shows that under such conditions the decay of Ca^{2+} transients was significantly enhanced in 7-week KO (compare Fig. 2*F*), and became

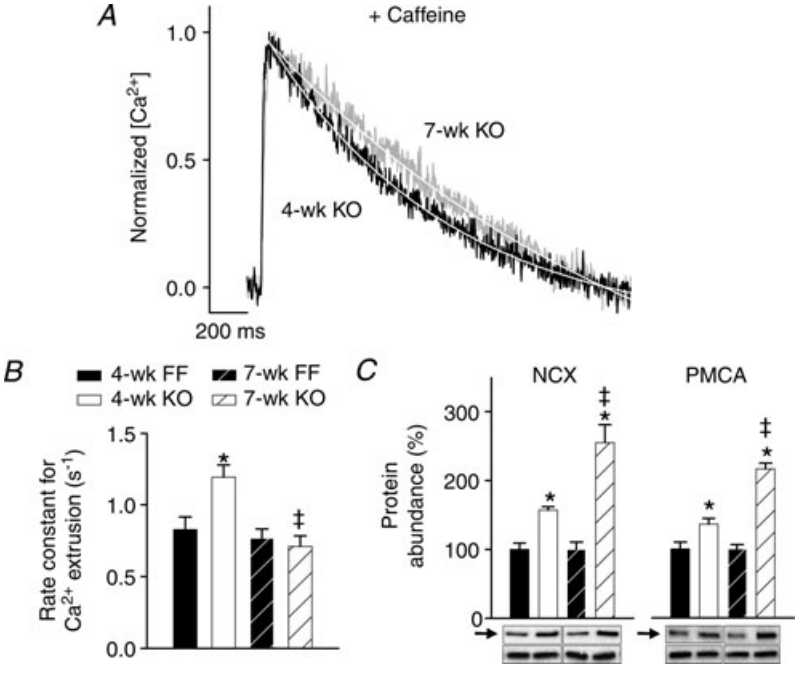

Figure 6. Ca^{2+} extrusion was enhanced in 4-week, but not 7-week KO
A, steady-state Ca^{2+} transients recorded in the presence of 10 mM caffeine. *B*, decay rate measurements. *C*, protein levels of NCX and PMCA (arrows) *vs.* calsequestrin (lower bands). (*n* for panels *B* and *C*: 4-week FF = 16, 5; 4-week KO = 18, 6; 7-week FF = 20, 6; 7-week KO = 18, 7; *$P < 0.05$ *vs.* equivalent FF, ‡$P < 0.05$ *vs.* equivalent 4-week).

even more rapid than in 4-week KO. These data support a detrimental role of Na^+ accumulation in promoting diastolic dysfunction in 7-week KO.

Discussion

In this study, we observed that mice with cardiomyocyte-specific ablation of SERCA2 developed end-stage HF by 7 weeks following knockout. Declining systolic and diastolic function between 4-week and 7-week KO was associated with reduction in cardiomyocyte contraction magnitude and slowing of relaxation, caused by parallel changes in Ca^{2+} transients. Progressive reduction in SR Ca^{2+} release was partially offset by AP prolongation, which increased L-type Ca^{2+} current, and by greater Ca^{2+} entry via reverse-mode NCX function. Diastolic dysfunction in end-stage HF resulted from a combination of declining SERCA activity and accumulation of intracellular Na^+ which impaired NCX-mediated Ca^{2+} extrusion. Increased $[Na^+]_i$ in 7-week KO was caused, at least in part, by down-regulation of NKA.

Elevation of $[Na^+]_i$ has been previously reported in both human HF (Pieske *et al.* 2002) and animal models (Despa *et al.* 2002; Baartscheer *et al.* 2003). The mechanisms proposed to underlie this Na^+ accumulation include increased late Na^+ current (Sossalla *et al.* 2008) and increased Na^+–H^+ exchange (Baartscheer *et al.* 2003). As well, in agreement with our observations, several previous studies have reported reduced NKA expression in failing myocytes (Schwinger *et al.* 1999; Muller-Ehmsen *et al.* 2001; Despa *et al.* 2002; Swift *et al.* 2008). Two of these studies have additionally reported decreased NKA activity (Schwinger *et al.* 1999; Swift *et al.* 2008). We observed reduced expression of both the α_1 and α_2 NKA isoforms. Based on our previous work (Swift *et al.* 2007),

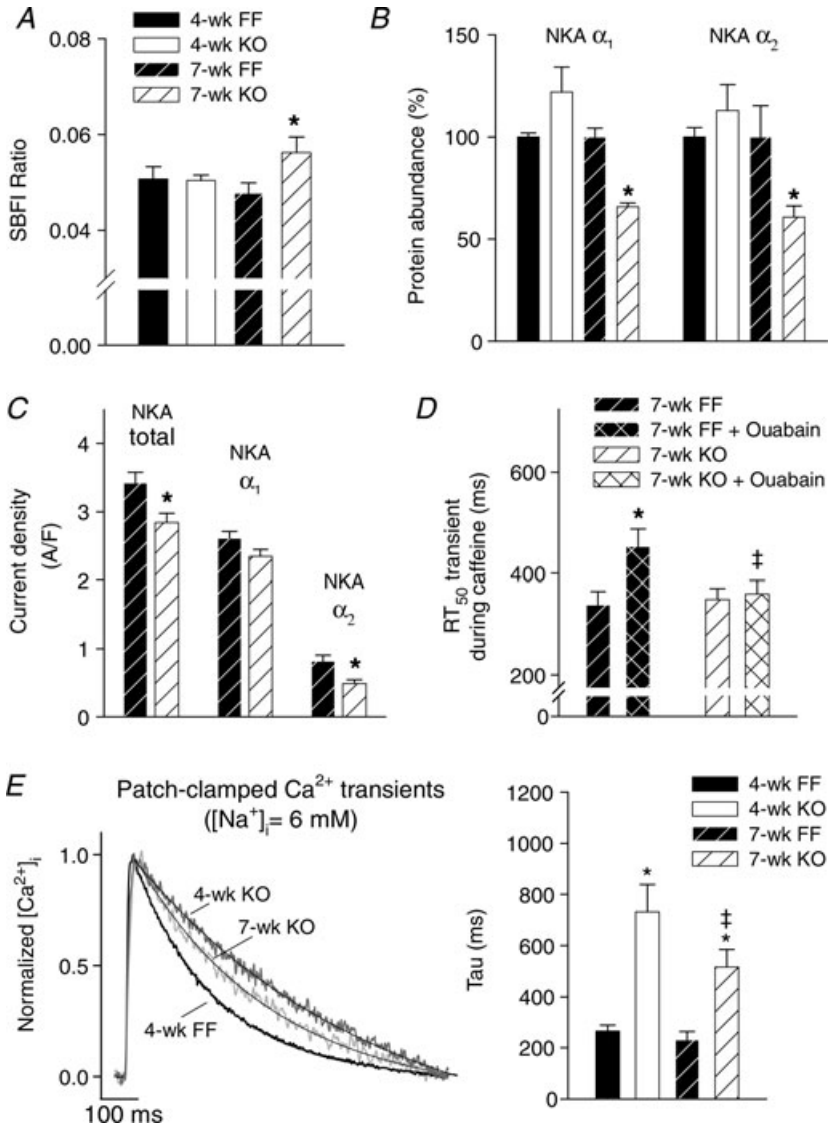

Figure 7. Elevated $[Na^+]_i$ impaired Ca^{2+} extrusion in 7-week KO
A, SBFI F_{410}/F_{590} ratios were increased in 7-week KO indicating cytosolic Na^+ accumulation ($n = 9, 9, 13, 10$ (order as in key here and in *E*)). *B*, expression of NKA α_1 and α_2 isoforms ($n = 6$ all groups). *C*, NKA currents obtained by rapid elevation of extracellular $[K^+]_i$ were subdivided into α_1 and α_2 components based on sensitivity to 5 μM ouabain (n for 7-week FF = 10, 7-week KO = 6). *D*, Ca^{2+} extrusion during NKA blockade by 1 mM ouabain, as estimated by half-decay time of Ca^{2+} transients during caffeine (n for 7-week FF = 10, 7-week KO = 10). *E*, Ca^{2+} transients following dialysis with 6 mM $[Na^+]_i$ ($n = 19, 11, 20, 19$). (For panels *A*–*C*, $^*P < 0.05$ *vs.* equivalent FF; panel *D*, $^*P < 0.05$ *vs.* untreated; ‡$P < 0.05$ *vs.* equivalent 7-week FF; panel *E*, $^*P < 0.05$ *vs.* equivalent FF, ‡$P < 0.05$ *vs.* equivalent 4-week).

we believe that the α_1 isoform plays a more important role in controlling global $[Na^+]$ than the α_2 isoform. With a reduction in α_1 expression, it might be hypothesized that remaining pumps could simply increase their activity to maintain normal $[Na^+]_i$. However, our preliminary data indicate that this is not the case, as we have observed that even partial blockade of the α_1 isoform results in increased $[Na^+]_i$. With reduced NKA pumping capacity, we postulate that $[Na^+]_i$ rises to a new steady-state level in 7-week KO, which stimulates remaining pumps, resulting in a normal rate of Na^+ extrusion to balance Na^+ influx. However, we actually measured reduced NKA current. This discrepancy is probably due to the fact that NKA current was measured in patch-clamped, dialysed cells which allowed comparison of pump current in KO and FF with $[Na^+]_i$ normalized. Interestingly, we observed that the α_2 component of the total NKA current was significantly decreased in 7-week KO. In our recent work, we have shown that the α_2 isoform is preferentially localized to the T-tubules, where it regulates local $[Na^+]$ near NCX (Swift *et al.* 2007). Therefore, it follows that down-regulation of α_2 in 7-week KO could impair NCX-mediated Ca^{2+} extrusion. Indeed, we observed that NKA blockade by ouabain treatment slowed Ca^{2+} extrusion in FF. Our finding that ouabain did not alter Ca^{2+} extrusion in KO suggests that Na^+ accumulation in the dyad may have maximally impaired forward-mode NCX in these cells.

PMCA function is believed to normally play a minor role in Ca^{2+} removal. However, data from the NCX knockout mouse indicate that the PMCA can have a surprisingly large capacity to extrude Ca^{2+} when challenged (Henderson *et al.* 2004). We presently observed a striking up-regulation of PMCA expression by more than 200% in 7-week KO, which would be expected to increase the rate of Ca^{2+} extrusion. As well, the Ca^{2+} affinity of PMCA might theoretically also be increased in KO myocytes, due to the action of regulatory molecules such as calmodulin (Brini, 2009). Thus, with NCX-mediated Ca^{2+} extrusion inhibited in these cells, PMCA may become an important mechanism for Ca^{2+} removal. In support of this view, we observed that in the presence of ouabain and high $[Na^+]_i$ (Swift *et al.* 2008), Ca^{2+} extrusion was significantly faster in 7-week KO than FF. Also, normalization of $[Na^+]_i$ by dialysis increased the rate of decay of 7-week KO Ca^{2+} transients beyond 4-week KO values. Therefore, with NCX function uninhibited, Ca^{2+} extrusion via NCX and PMCA may be able to maintain diastolic function at near-normal levels in the complete absence of SERCA function.

The mechanisms that compensate for declining SR Ca^{2+} content and release are intriguing. We previously reported up-regulation of the L-type Ca^{2+} channel and increased Ca^{2+} current magnitude in 4-week KO myocytes (Andersson *et al.* 2009*a*). We presently confirmed these findings, and observed that increases in Ca^{2+} channel expression and current magnitude persist in 7-week KO. In fact, integrated currents tended to be even larger in 7-week than 4-week KO. Our AP clamp experiments showed that the longer AP in 7-week KO additionally facilitated L-type Ca^{2+} current, resulting in Ca^{2+} currents that were 3- to 3.5-fold larger than those recorded in FF cells during FF APs. Additional Ca^{2+} current during the prolonged AP substantially increased Ca^{2+} transient magnitude in 7-week KO. However, these effects were more modest in FF cells, which have functional SR, since AP prolongation is known to reduce the efficiency of Ca^{2+}-induced Ca^{2+} release (Sah *et al.* 2003). Ca^{2+} currents may have been additionally enhanced in 7-week KO by Ca^{2+}–calmodulin-dependent kinase II phosphorylation, as has been reported in other heart failure models (Wang *et al.* 2008).

AP prolongation might also be expected to enhance Ca^{2+} entry via reverse-mode NCX. However, we observed that the 7-week KO AP induced a similar increase in Ca^{2+} transient magnitude in the presence and absence of KB-R7943. It appears then that the benefits of AP prolongation in 7-week KO mice stem primarily from greater L-type Ca^{2+} current. Compared to the untreated condition, however, Ca^{2+} transient magnitude was decreased by KB-R7943 in 7-week KO, but unaltered in 7-week FF. This suggests that NCX-mediated Ca^{2+} entry is enhanced in KO on a beat-to-beat basis, as predicted when Na^+ levels are increased and Ca^{2+} transients are reduced. At the tested dose of 5 μM, KB-R7943 is reported to block 90% of reverse-mode NCX function without reducing forward-mode activity (Satoh *et al.* 2000). Although some have suggested that KBR is not mode-selective, recent evidence indicates that bi-modal NCX blockade increases Ca^{2+} transient magnitude (Ozdemir *et al.* 2008). We observed that KBR *reduced* transient magnitude and did not alter decay kinetics (data not shown), indicating preferential reverse-mode blockade.

Despite markedly enhanced Ca^{2+} influx, declining SR function resulted in a progressive reduction in Ca^{2+} transient amplitude in KO cells, which was observed at both low and high stimulation frequency (1 Hz and 6 Hz). Four-week KO myocytes also exhibited reduced contraction magnitudes at 1 Hz, but contractile function was enhanced at high pacing rates as 6 Hz contractions were similar in magnitude to controls. This is in agreement with our previous observation that myofilament responsiveness to Ca^{2+} is increased in 4-week KO (Andersson *et al.* 2009*a*), which may become particularly pronounced at high stimulation rates when diastolic $[Ca^{2+}]_i$ is elevated. In addition, the slowed Ca^{2+} transient kinetics in KO may also improve contractile function by prolonging myofilament activation. Such alterations may continue to aid contractile function in 7-week KO, as contraction magnitude was increased between 1 Hz and 6 Hz despite the presence of very

small Ca^{2+} transients at both frequencies. Nevertheless, it appears that such adaptations are insufficient to maintain systolic function at normal levels at this late time point when SR function fails completely.

Although there are clearly important differences between end-stage heart failure in humans and SERCA2 KO mice, some cellular mechanisms may be conceptually similar. Data from human HF appear to support our observation that slowing of Ca^{2+} extrusion is an important mechanism underlying diastolic dysfunction. Hasenfuss *et al.* (1999) observed that HF patients with impaired diastolic performance exhibited decreased SERCA expression but unchanged NCX. In contrast, NCX levels were increased in patients with preserved diastolic function. The authors suggested that greater NCX activity may compensate for reduced SERCA function to maintain near-normal Ca^{2+} decay and relaxation rates. Our results also support the notion that reduction in SERCA levels can promote systolic dysfunction. In human HF, SERCA expression is often reported to be reduced by 30–40% (for review, see Hasenfuss & Pieske, 2002), and this reduction is generally believed sufficient to impair systolic performance. Mice are clearly very adept at compensating for loss of SERCA, since we observed near-normal systolic function in 4-week KO despite a more than 95% reduction in SERCA2a protein. We have previously shown that activation of the sympathetic nervous system contributes to this compensation (Andersson *et al.* 2009*a*). In the present study, we observed that loss of a small remaining pool of SERCA2a by 7-week KO was associated with development of systolic HF. Since the half-life for SERCA protein is approximately 2–3 days (Andersson *et al.* 2009*a*), it is surprising that a functional amount of SERCA would be present beyond the first few weeks following knockout. However, it may be that there is normally an excessive amount of SERCA protein, much of which is either not required or not accessible for normal function. Alternatively, there may be two different pools of SERCA protein: one pool which has a short half-life, and a second perhaps smaller pool which has a longer half-life. Theoretically, declining SERCA activity between 4- and 7-week KO could result from gradual loss of this second pool of SERCA protein.

Compensatory mechanisms present in KO myocytes may not be present in human HF. For example, Ca^{2+} current is generally reported to be unaltered in failing human myocytes (Bers, 2006). As well, more profound AP prolongation in human HF is believed to reduce, not augment, Ca^{2+} transient magnitude (Sah *et al.* 2003). Therefore, relatively moderate reductions in SERCA expression such as those reported in HF patients may be sufficient to impair systolic function if Ca^{2+} influx is not increased. Our findings suggest then that strategies aimed at enhancing Ca^{2+} influx may be beneficial in treating systolic dysfunction. Diastolic function, on the other hand, would probably benefit from augmentation of NKA activity and Na^+ unloading. Such therapies may, however, have the opposite effect on systolic function, since elevated $[Na^+]_i$ is known to increase Ca^{2+} transients by elevating SR Ca^{2+} load. Indeed, clinical trials have indicated that digoxin, a NKA inhibitor, is appropriate for treatment of systolic but not diastolic dysfunction in HF (Shammas *et al.* 2007). A therapeutic compromise may be attainable through agents such as istaroxime, a newly developed compound which simultaneously inhibits NKA and stimulates SERCA. Early clinical data suggest that istaroxime improves both contractility and diastolic relaxation in HF patients (Khan *et al.* 2009).

In conclusion, our data from the SERCA KO mouse indicate that declining SERCA function in end-stage HF contributes to the simultaneous development of both systolic and diastolic dysfunction. However, impaired relaxation also results from accumulation of intracellular Na^+ following down-regulation of NKA. Our data indicate that Ca^{2+} extrusion mechanisms can dramatically compensate for SERCA loss to maintain diastolic function when Na^+ gain is prevented.

References

Andersson KB, Birkeland JA, Finsen AV, Louch WE, Sjaastad I, Wang Y, Chen J, Molkentin JD, Chien KR, Sejersted OM & Christensen G (2009*a*). Moderate heart dysfunction in mice with inducible cardiomyocyte-specific excision of the *Serca2* gene. *J Mol Cell Cardiol* **47**, 180–187.

Andersson KB, Finsen AV, Sjåland C, Winer LH, Sjaastad I, Ødegaard A, Louch WE, Wang Y, Chen J, Chien KR, Sejersted OM & Christensen G (2009*b*). Mice carrying a conditional *Serca2^{flox}* allele for the generation of Ca^{2+} handling-deficient mouse models. *Cell Calcium* **46**, 219–225.

Andersson KB, Winer LH, Mork HK, Molkentin JD & Jaisser F (2009*c*). Tamoxifen administration routes and dosage for inducible Cre-mediated gene disruption in mouse hearts. *Transgenic Res* DOI: 10.1007/s11248-009-9342-4.

Baartscheer A, Schumacher CA & Fiolet JW (1997). Small changes of cytosolic sodium in rat ventricular myocytes measured with SBFI in emission ratio mode. *J Mol Cell Cardiol* **29**, 3375–3383.

Baartscheer A, Schumacher CA, van Borren MM, Belterman CN, Coronel R & Fiolet JW (2003). Increased Na^+/H^+-exchange activity is the cause of increased $[Na^+]_i$ and underlies disturbed calcium handling in the rabbit pressure and volume overload heart failure model. *Cardiovasc Res* **57**, 1015–1024.

Berry RG, Despa S, Fuller W, Bers DM & Shattock MJ (2007). Differential distribution and regulation of mouse cardiac Na^+/K^+-ATPase $\alpha 1$ and $\alpha 2$ subunits in T-tubule and surface sarcolemmal membranes. *Cardiovasc Res* **73**, 92–100.

Bers DM (2001). *Excitation-Contraction Coupling and Cardiac Contractile Force*. Kluwer Academic Publishers, Dordrecht, The Netherlands.

Bers DM (2006). Altered cardiac myocyte Ca regulation in heart failure. *Physiology (Bethesda)* **21**, 380–387.

Brini M (2009). Plasma membrane Ca^{2+}-ATPase: from a housekeeping function to a versatile signalling role. *Pflugers Arch* **457**, 657–664.

Campbell AM, Wuytack F & Fambrough DM (1993). Differential distribution of the alternative forms of the sarcoplasmic/endoplasmic reticulum Ca^{2+}-ATPase, SERCA2b and SERCA2a, in the avian brain. *Brain Res* **605**, 67–76.

Cheng H, Lederer WJ & Cannell MB (1993). Calcium sparks: elementary events underlying excitation-contraction coupling in heart muscle. *Science* **262**, 740–744.

Despa S, Islam MA, Weber CR, Pogwizd SM & Bers DM (2002). Intracellular Na^+ concentration is elevated in heart failure but Na/K pump function is unchanged. *Circulation* **105**, 2543–2548.

Drummond GB (2009). Reporting ethical matters in *The Journal of Physiology*: standards and advice. *J Physiol* **587**, 713–719.

Everts ME, Andersen JP, Clausen T & Hansen O (1989). Quantitative determination of Ca^{2+}-dependent Mg^{2+}-ATPase from sarcoplasmic reticulum in muscle biopsies. *Biochem J* **260**, 443–448.

Finsen AV, Christensen G & Sjaastad I (2005). Echocardiographic parameters discriminating myocardial infarction with pulmonary congestion from myocardial infarction without congestion in the mouse. *J Appl Physiol* **98**, 680–689.

Hasenfuss G & Pieske B (2002). Calcium cycling in congestive heart failure. *J Mol Cell Cardiol* **34**, 951–969.

Hasenfuss G, Schillinger W, Lehnart SE, Preuss M, Pieske B, Maier LS, Prestle J, Minami K, Just H (1999). Relationship between Na^+-Ca^{2+}-exchanger protein levels and diastolic function of failing human myocardium. *Circulation* **99**(5), 641–648.

Henderson SA, Goldhaber JI, So JM, Han T, Motter C, Ngo A, Chantawansri C, Ritter MR, Friedlander M, Nicoll DA, Frank JS, Jordan MC, Roos KP, Ross RS & Philipson KD (2004). Functional adult myocardium in the absence of Na^+-Ca^{2+} exchange: cardiac-specific knockout of NCX1. *Circ Res* **95**, 604–611.

Iwamoto T, Watano T & Shigekawa M (1996). A novel isothiourea derivative selectively inhibits the reverse mode of Na^+/Ca^{2+} exchange in cells expressing NCX1. *J Biol Chem* **271**, 22391–22397.

Khan H, Metra M, Blair JE, Vogel M, Harinstein ME, Filippatos GS, Sabbah HN, Porchet H, Valentini G & Gheorghiade M (2009). Istaroxime, a first in class new chemical entity exhibiting SERCA-2 activation and Na-K-ATPase inhibition: a new promising treatment for acute heart failure syndromes? *Heart Fail Rev* **14**, 277–287.

Louch WE, Mork HK, Sexton J, Stromme TA, Laake P, Sjaastad I & Sejersted OM (2006). T-tubule disorganization and reduced synchrony of Ca^{2+} release in murine cardiomyocytes following myocardial infarction. *J Physiol* **574**, 519–533.

Mork HK, Sjaastad I, Sejersted OM & Louch WE (2009). Slowing of cardiomyocyte Ca^{2+} release and contraction during heart failure progression in post-infarction mice. *Am J Physiol Heart Circ Physiol* **296,** H1069–H1079.

Muller-Ehmsen J, Wang J, Schwinger RH & McDonough AA (2001). Region specific regulation of sodium pump isoform and Na,Ca-exchanger expression in the failing human heart – right atrium vs left ventricle. *Cell Mol Biol (Noisy -le-grand)* **47**, 373–381.

Ozdemir S, Bito V, Holemans P, Vinet L, Mercadier JJ, Varro A & Sipido KR (2008). Pharmacological inhibition of Na/Ca exchange results in increased cellular Ca^{2+} load attributable to the predominance of forward mode block. *Circ Res* **102**, 1398–1405.

Pieske B, Maier LS, Piacentino V III, Weisser J, Hasenfuss G & Houser S (2002). Rate dependence of $[Na^+]_i$ and contractility in nonfailing and failing human myocardium. *Circulation* **106**, 447–453.

Pogwizd SM, Schlotthauer K, Li L, Yuan W & Bers DM (2001). Arrhythmogenesis and contractile dysfunction in heart failure: roles of sodium-calcium exchange, inward rectifier potassium current, and residual β-adrenergic responsiveness. *Circ Res* **88**, 1159–1167.

Sah R, Ramirez RJ, Oudit GY, Gidrewicz D, Trivieri MG, Zobel C & Backx PH (2003). Regulation of cardiac excitation–contraction coupling by action potential repolarization: role of the transient outward potassium current (I_{to}). *J Physiol* **546**, 5–18.

Satoh H, Ginsburg KS, Qing K, Terada H, Hayashi H & Bers DM (2000). KB-R7943 block of Ca^{2+} influx via Na^+/Ca^{2+} exchange does not alter twitches or glycoside inotropy but prevents Ca^{2+} overload in rat ventricular myocytes. *Circulation* **101**, 1441–1446.

Schwinger RH, Wang J, Frank K, Muller-Ehmsen J, Brixius K, McDonough AA & Erdmann E (1999). Reduced sodium pump α1, α3, and β1-isoform protein levels and Na^+,K^+-ATPase activity but unchanged Na^+-Ca^{2+} exchanger protein levels in human heart failure. *Circulation* **99**, 2105–2112.

Shammas RL, Khan NU, Nekkanti R & Movahed A (2007). Diastolic heart failure and left ventricular diastolic dysfunction: what we know, and what we don't know! *Int J Cardiol* **115**, 284–292.

Sossalla S, Wagner S, Rasenack EC, Ruff H, Weber SL, Schondube FA, Tirilomis T, Tenderich G, Hasenfuss G, Belardinelli L & Maier LS (2008). Ranolazine improves diastolic dysfunction in isolated myocardium from failing human hearts – role of late sodium current and intracellular ion accumulation. *J Mol Cell Cardiol* **45**, 32–43.

Swift F, Birkeland JA, Tovsrud N, Enger UH, Aronsen JM, Louch WE, Sjaastad I & Sejersted OM (2008). Altered Na^+/Ca^{2+}-exchanger activity due to downregulation of Na^+/K^+-ATPase α2-isoform in heart failure. *Cardiovasc Res* **78**, 71–78.

Swift F, Tovsrud N, Enger UH, Sjaastad I & Sejersted OM (2007). The Na^+/K^+-ATPase α2-isoform regulates cardiac contractility in rat cardiomyocytes. *Cardiovasc Res* **75**, 109–117.

Thomas MJ, Sjaastad I, Andersen K, Helm PJ, Wasserstrom JA, Sejersted OM & Ottersen OP (2003). Localization and function of the Na^+/Ca^{2+}-exchanger in normal and detubulated rat cardiomyocytes. *J Mol Cell Cardiol* **35**, 1325–1337.

Wang Y, Tandan S, Cheng J, Yang C, Nguyen L, Sugianto J, Johnstone JL, Sun Y & Hill JA (2008). Ca^{2+}/calmodulin-dependent protein kinase II-dependent remodelling of Ca^{2+} current in pressure overload heart failure. *J Biol Chem* **283**, 25524–25532.

Author contributions

Conception and design of this study was conducted by W.E.L, I.S., K.B.A., G.C. and O.M.S. Experiments examining cardiomyocyte size, contractile function, Ca^{2+} and Na^{+} homeostasis, and action potential configuration, were performed by W.E.L., H.K.M., F.S. and J.M.A. Cardiomyocyte isolation was conducted by K.H. Echocardiographic analysis was performed by K.H. and I.S. Morphological and histological examinations were conducted by K.B.A., H.M.R. and B.R. Kaplan Meyer curves and LV Ca^{2+}-ATPase activity were determined by K.B.A. All authors contributed to writing of the manuscript.

Acknowledgements

We thank Annlaug Ødegård, Ulla Enger, Heidi Kvaløy, and Tove Norén for excellent technical assistance. This work was supported by The Research Council of Norway (W.E.L, H.K.M.); The South-Eastern Norway Regional Health Authority (F.S.); Anders Jahre's Fund for the Promotion of Science; Oslo University Hospital Ullevaal (I.S., K.B.A., G.C., O.M.S.); and the University of Oslo (G.C., O.M.S.).